Research Article

Syed M. Hussain, Mohamed R. Eid*, M. Prakash, Wasim Jamshed, Abbas Khan, and Haifa Alqahtani

Thermal characterization of heat source (sink) on hybridized (Cu–Ag/EG) nanofluid flow via solid stretchable sheet

https://doi.org/10.1515/phys-2022-0245
received July 16, 2022; accepted April 19, 2023

Abstract: The goal of this research is to consider the thermal impact on varied convection flow in hybrid nanofluids with heat generation over a two-dimensional heated flat around a stretchable sheet. The flow is considered steady and incompressible while the stretchable sheet is assumed an impermeable. Two distinctive nano-level particles are considered, namely copper (Cu) and silver (Ag) with ethylene glycol base fluid. The boundary layer was generated on a stretchable sheet surface by mixed convection flow in hybrid nanofluids. Ideally, the sink and source are thermal reservoirs of internal thermal capacities. This means you can extract or reject heat from them without changing their temperature. To make a study of thermodynamic systems like heat engines and refrigerator systems, the governing equations were solved numerically with Keller-box methodology depending on the implicit finite-difference technique. Research findings were worked with the parameters of mixed convection, Prandtl number, nanoparticle volume fraction, through various non-dimensional parameters, and heat generation. Especially for thermal generation enhancement, the fluidity and thermal dispersal get elevated. Even though the flowing behavior and the thermal dispersal of hybridity fluids with the combinations of Cu and Ag nanoparticles were similar, their values are distinct, which reflect in graphical displays. The hybrid nanofluidity gets improved with the volume variation of nanoparticles if the ϕ value is $0.01 \le \phi \le 0.05$ and if the flow profile value decreases ϕ_h, where $0.01 \le \phi_h \le 0.05$ as the dispersal of temperature enhances when the nanoparticle nanofluid constraint is improved.

Keywords: hybrid nanofluid, heat generating, nanoparticles, non-permeable stretchable sheet, mixed convection

Nomenclature

a,b	constants
Ag	silver
c	material parameter
Cu	copper
C_p	heat capacitance (J/K)
f	non-dimensional rapidity
k	thermal conductance (W/m K)
Pr	Prandtl quantity
Q_0	heat generating (sinking) (J)
Q	source of heat
s	suction
T	temperature (K)
u, v	rapidity components (m/s)
x, y	Cartesian coordinates (m)

Greek symbols

α	thermal diffusivity (m^2/s)
β	thermal expansion (1/K)
η	similarity parameter
θ	non-dimensional temperature
λ	mixed convective variable

* **Corresponding author: Mohamed R. Eid,** Department of Mathematics, Faculty of Science, New Valley University, Al-Kharga, Al-Wadi Al-Gadid, 72511 Egypt; Department of Mathematics, Faculty of Science, Northern Border University, Arar, 1321, Saudi Arabia, e-mail: m_r_eid@yahoo.com
Syed M. Hussain: Department of Mathematics, Faculty of Science, Islamic University of Madinah, Madinah, 42351, Saudi Arabia
M. Prakash: Department of Mathematics, KPR Institute of Engineering and Technology, Coimbatore, India
Wasim Jamshed: Department of Mathematics, Capital University of Science and Technology (CUST), Islamabad, 44000, Pakistan
Abbas Khan: Department of Mathematics, University of Haripur, Haripur, 22620, Khyber Pakhtunkhwa, Pakistan
Haifa Alqahtani: Department of Analytics in the Digital Era, College of Business and Economics, United Arab Emirates University, Madinah, United Arab Emirates

μ	dynamic viscid (Pa s)
ρ	density (kg/m^3)
υ	kinematic viscid (m^2/s)
ϕ	volume of nanoparticle
ϕ_h	volume of hybrid nanoparticle
ϕ_1	copper nanomolecule size
ϕ_2	silver nanomolecule size

Subscripts

0	initial condition
w	wall
∞	free condition
f	fluid
nf	nanofluid
hnf	hybridity nanofluid

1 Introduction

Complicated phenomena modeling to comprehend the fundamental physics between them is a developing and helpful tool for academics, scientists, and engineers. Numerous significant empirical relationships have been undertaken and proposed in order to model the nature of complicated phenomena originating in physical sciences. Ideally, the sink and source are thermal reservoirs of internal thermal capacities. This means you can extract or reject heat from them without changing their temperature. Practically, such a device does not exist; these are just concepts to study thermodynamic systems such as heat engines and refrigerator systems. If the reservoir continuously supplies heat energy to the system, it is a source, whereas if the reservoir continuously absorbs heat energy from the system, it is a sink.

Energy saving is a crucial concern in several sophisticated industrial and technological applications using heat transfer technologies. Conservative fluids, such as polymeric solution, biological fluids, glycols, water, triethylene refrigerants, ethylene, oils, and lubricants, have been used as heat transfer fluids for many decades. In several engineering disciplines, such as polymer extrusions, rapidly cooling, glass blowing, refrigeration of microelectronics, deep drawing, and extinction in metalworks, the survey of flowing and heat transference over a stretchable sheet has been in high demand during the last few years. Crane [1] initiated the exploration of the boundary layer flow across stretched materials. Ever since, previous scholars [2,3] have come forth to contribute to work on various areas of flowing and heat transfer issues requiring stretched materials.

The primary issue for current science and technology is to improve the heat transfer rate of traditional base fluids – to increase thermal performing and refrigeration systems such as refrigeration circuits boarding, heat transfer, and automobile refrigerating systems with the highest thermal efficacy, temperature lessening, detailed functioning capability, and tinned span. Because of this, researchers and scientists were drawn to investigate the heat transport characteristics of fine materials in comparison to traditional base fluids. Likewise, nanomaterials are a distinct form of fluid that contain a combination of solid nanoparticles with sizes of 100 nm or less and standard base fluids. Metallic solids such as Cu, Al, Ag, and Au, non-metallic solids (SiO_2, Al_2O_3, carbides, and nanotubes), and metallic liquids are all present in such liquids (sodium alginate). Water, paraffin, motor oil, benzene, ethylene, and tri-ethylene glycol are examples of ordinary base liquids. Due to their better thermal conductivity than base liquids, nanomaterials are utilized as improved coolants in processors and nuclear reactors, pharmacological treatments, safer operations, lubrication, heat exchange, and micro-channel passive heatsinks. Similar liquids are also generally utilized in a variety of electrical appliances used in military sectors, cars, and converters, as well as in the construction of waste heat removal equipment. Because of their high heat transfer capabilities, such liquids are used in a collection of production implementations, comprising chemicals and substances, oil and gas, nutrition/food safety, newspaper and printers, and transports. In the flowing analysis, Hamilton and Crosser [4] and Maxwell [5] mathematically built their formulations explaining rheological properties while taking the structure of the nanomaterials into consideration. It was ironic that Choi [6] was the first to perform experimental research and expose to society the improved thermal conducting of fluids using nanomaterials. Khan and Pop [7] went on to design the boundary layer flowing of nanoliquids across a stretched plane. Mabood *et al.* [8] discovered that in the absence and existence of magnetization, Al_2O_3–water nanofluid contributes to a larger impetus bounder layer than Cu–water nanofluid. Hayat *et al.* [9] studied the non-linear radioactive heating influences of Ag and Cu nanomolecules in conjunction with combined convection using water as the base liquid. In their work, they discovered that adding an irradiation variable decreases the mean absorbing factor, which increases the heat transference rate, resulting in increased cooling in both Cu–H_2O and Ag–H_2O nanoliquids [10]. In their work, Du and Tang [11]

investigated the photosensitive characteristics of plasmonic nanoliquids that contain Au nanomolecules of various forms, volumes, phase ratio, and concentricities. Furthermore, the study by Du and Tang [12] investigated the effects of particle aggregation, particle diameter, and particle fractional size on the absorbance values of nanoliquids in their work. There are some recent research articles on nanofluid under various physical situations [13–15].

Nanofluids play a significant role in heat transmission mechanisms because of their observable properties that may be reformed as desired. Furthermore, nanofluids have received a lot of interest due to their broad use in sectors including paper, pharmaceuticals, and medicine. To improve the heat transference abilities of nanoliquids, investigators developed a novel kind of nanoliquid known as a hybridized nanoliquid. Hybrid nanofluids are a relatively new idea that offers several advantages over regular nanofluids. While selecting the optimum nanomolecule combination, an aggregation analysis of the nanomolecules is required. The main challenge in the field of hybridized nanofluids is the instability of hybridized nanomolecules in base fluids. Anjali Devi and Devi [16,17] began early-stage numerical hybrid nanofluid research in the bounder-layer characterization. Eid and Nafe [18] later investigated the heat source and slip effects of the hybridized nanofluid in magnetohydrodynamics (MHD) setting. Following them, various study data were published to support the advantages of hybridized nanofluids in a variety of situations [19–21]. The dispersal of many nanomaterials inside the base liquid results in hybridized nanofluids. These nanomolecules improve the thermal properties of the liquid. Hybridity nanoliquids are used to achieve the desired rate of heat transport and nanomolecule numbers. These liquids have a variety of thermal management applications, including naval constructions, healthcare, micro-fluidics, defense, transportations, and construction. Eastman *et al.* [22] investigated the thermal conductance of fluids modified by Cu and carbon nanotubes in conventional liquid and without them. Suresh *et al.* [23] investigated the experimental fabrication of a hybridized nanofluid including CuO and Al nanomolecules. Suresh *et al.* [24] investigated the thermal characteristics of nanoliquid Al_2O_3–Cu/water. Sarkar *et al.* [25] examined hybridized nanomaterial inspection and production. Hassan *et al.* [26] investigated the heat transmission of hybridized nanomaterials including Cu–Ag/H_2O nanomolecules. Dinarv and Pop [27] investigated nanostructured materials' rotational convection *via* a cone. Acharya [28] investigated a hybrid nanofluid over a square enclosure having variously shaped multiple heated obstacles. Acharya [29] investigated the hydrothermal and entropy aspects of buoyancy-driven MHD hybridity nanoliquid flowing inside an octagonal area. Acharya and Chamkha [30] investigated Al_2O_3–water-based hybrid flow through parallel fins surrounded by a partially heated hexagonal cavity.

Khan *et al.* [31] investigated the effect of three distinct nanomolecules on the flowing of the Cattaneo–Christov heating flux prototype across an exponentially plate. Waini *et al.* [32] investigated the heat transference of a hybridized nanoliquid flowing on a stretchable plate with a regular shearing flux. Ahmad and Nadeem [33] investigated the entropy production and temperature-dependent viscid of single walled carbon nanotubes–multi-walled carbon nanotubes hybridized nanofluid flowing. Lund *et al.* [34] probed the combined solution and stableness assessment of hybridity nanoliquid using a diminishing plate effect of viscidness dissipative flowing. Waini *et al.* [35] investigated the constant flowing of a hybridized nanoliquid in the existence of porousness media throughout a vibrating thin needle. According to Mozafari *et al.* [36], the size-centering process necessitates a dependency on the rate of growth on the size of nanomolecules and the saturation of the compounds on the nanomolecule surfaces. Many studies have explored the characteristics [37–39].

To the best of the authors' awareness, no research attempts were made to examine the thermal source (sink) effects of mixed, convectively flowing hybridized nanofluid passes over the impermeable stretchable sheet. With this confidence, the authors numerically worked using the Keller-box methodology, which is dependent on the implicit finite difference technique with Cu and Ag suspensions. Figure 1 presents the scheme diagram of the flowing representation.

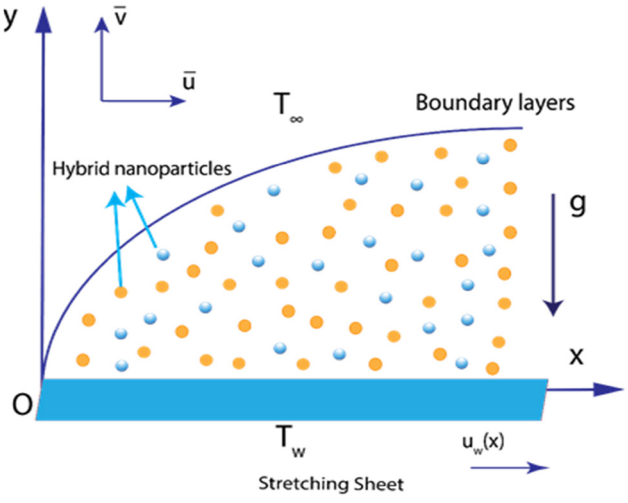

Figure 1: Flow system diagram.

2 Mathematical formulation

First, the mathematical models were developed by deriving from the conservation equation of mass, momentum, and energy. From this, the continuity equation, motion equation, and energy equation were obtained [3,9].

$$\frac{\partial \bar{u}}{\partial \bar{x}} + \frac{\partial \bar{v}}{\partial \bar{y}} = 0, \tag{1}$$

$$\left(\bar{u}\frac{\partial \bar{u}}{\partial \bar{x}} + \bar{v}\frac{\partial \bar{u}}{\partial \bar{y}}\right) = -u_e\frac{du_e}{dx} + \frac{\mu_{hnf}}{\rho_{hnf}}\left(\frac{\partial^2 \bar{u}}{\partial \bar{x}^2}\right) + \frac{(\rho\beta)_{hnf}}{\rho_{hnf}}(\bar{T} - T_\infty)g, \tag{2}$$

$$\left(\bar{u}\frac{\partial \bar{T}}{\partial \bar{x}} + \bar{v}\frac{\partial \bar{T}}{\partial \bar{y}}\right) = \alpha_{hnf}\left(\frac{\partial^2 \bar{T}}{\partial \bar{y}^2}\right) + \frac{Q_0}{(\rho_{C_p})_{hnf}}(\bar{T} - T_\infty), \tag{3}$$

and the following are the associated boundary conditions for presenting the flow [9].

$$\bar{u} = 0, \bar{v} = v_w(x), \bar{T} = 0 \quad \text{at} \quad y = 0, \tag{4}$$

$$\bar{u} \to u_w(x), \quad \bar{T} \to T_w(x) = T_\infty + T_0 x \quad \text{as} \quad y \to \infty. \tag{5}$$

where ref. [19]

$$\mu_{hnf} = \mu_f(1 - \phi_1 - \phi_2)^{-2.5}, \tag{6}$$

$$\rho_{hnf} = \phi_1\rho_1 + \phi_2\rho_2 + (1 - \phi_h)\rho_f, \tag{7}$$

$$\beta_{hnf} = \phi_1\beta_1 + \phi_2\beta_2 + (1 - \phi_h)\beta_f, \tag{8}$$

$$\alpha_{hnf} = \frac{k_{hnf}}{(\rho C_p)_{hnf}}, \tag{9}$$

$$(\rho C_p)_{hnf} = \phi_1(\rho C_p)_1 + \phi_2(\rho C_p)_2 + (1 - \phi_h)(\rho C_p)_f, \tag{10}$$

$$k_{hnf} = \left\{\frac{\phi_1 k_1 + \phi_2 k_2}{\phi_h} + 2k_f + 2(\phi_1 k_1 + \phi_2 k_2) - 2\phi_h k_f\right\} \times \left\{\frac{\phi_1 k_1 + \phi_2 k_2}{\phi_h} + 2k_f - (\phi_1 k_1 + \phi_2 k_2) + (1 - \phi_h)k_f\right\}^{-1}, \tag{11}$$

where $\phi_h = \phi_1 + \phi_2$. Now introducing non-dimensional variables, we obtain [3,9]

$$\left.\begin{aligned} u_w(x) &= bx, \\ u_e(x) &= ax, \\ v_w(x) &= -\sqrt{a\upsilon_f}\,s, \\ \bar{u} &= axf'(\eta), \\ \bar{v} &= -\sqrt{a\upsilon_f}\,f(\eta), \\ \theta(\eta) &= \frac{\bar{T} - T_\infty}{T_w - T_\infty}, \\ \eta &= \sqrt{\frac{a}{\upsilon_f}}\,y, \\ T_w(x) &= T_\infty + T_0 x. \end{aligned}\right\} \tag{12}$$

In this equation, a and b are constants, s is the suction parameter, and T_0 is the constant characteristic temperature.

Eq. (1) is thus met exactly by the specified similarity transformation in Eq. (12). We obtain the following combined non-linearly ordinary differential equations by putting similarity conversion in Eq. (12) into expressions in Eqs. (2) and (3).

$$1 - (f')^2 + ff' + \frac{\phi_a}{\phi_b}(f''') + \frac{\phi_c}{\phi_b}\lambda\theta = 0, \tag{13}$$

$$f\theta' + \frac{1}{\Pr}\phi_g\theta'' + \frac{1}{\phi_d}Q\theta = 0, \tag{14}$$

where λ denotes the mixed convection constraint, Pr symbolizes the Prandtl quantity, and Q signifies the source of heat constraint.

Concerning the boundary constraints,

$$\left.\begin{aligned} f = s, f' &= 0, \\ \theta = 0 \quad \text{at} \quad y &= 0, \\ f' \to 1; \theta \to 1 \quad \text{as} \quad y &\to \infty. \end{aligned}\right\} \tag{15}$$

The parameters Pr, λ, Q, s, and c can be expressed in the following equations:

$$\Pr = \frac{1}{\alpha_f}\frac{\mu_f}{\rho_f}, \lambda = \frac{\mathrm{Gr}}{\mathrm{Re}^2}, \mathrm{Gr} = \frac{g\beta_f(T_w - T_\infty)a^3\rho_f^2}{\mu_f^2}, \quad Q = \frac{Q_0}{a(\rho C_p)_{hnf}}, s = \frac{v_w(x)}{a\upsilon_f}, c = \frac{b}{a}, \tag{16}$$

where

$$\phi_a = \frac{\mu_{hnf}}{\mu_f} = (1 - \phi_1 - \phi_2)^{-2.5}, \tag{17}$$

$$\phi_b = \frac{\rho_{hnf}}{\rho_f} = \frac{1}{\rho_f}(\phi_1\rho_1 + \phi_2\rho_2) + (1 - \phi_h)\rho_f, \tag{18}$$

$$\phi_c = \frac{(\rho\beta)_{hnf}}{\rho_f\beta_f} = \frac{1}{\rho_f\beta_f}(\phi_1\beta_1 + \phi_2\beta_2) + (1 - \phi_h)\beta_f, \tag{19}$$

$$\phi_d = \frac{(\rho C_p)_{hnf}}{(\rho C_p)_f} = \frac{1}{(\rho C_p)_f}[\phi_1(\rho C_p)_1 + \phi_2(\rho C_p)_2] + (1 - \phi_h)(\rho C_p)_f, \tag{20}$$

$$\phi_e = \frac{k_{hnf}}{k_f} = \frac{1}{k_f}\left\{\frac{\phi_1 k_1 + \phi_2 k_2}{\phi_h} + 2k_f + 2(\phi_1 k_1 + \phi_2 k_2) - 2\phi_h k_f\right\} \times \left\{\frac{\phi_1 k_1 + \phi_2 k_2}{\phi_h} + 2k_f - (\phi_1 k_1 + \phi_2 k_2) + (1 - \phi_h)k_f\right\}^{-1}, \tag{21}$$

$$\phi_g = \frac{\alpha_{hnf}}{(\rho C_p)_{hnf}}. \tag{22}$$

Table 1: Nanofluid thermophysical materials

Coefficient in physics	EG (base fluid)	Cu	Ag
C_p (kg/m^3)	2,417	385	235
ρ (kg/m^3)	110.7	8,933	10,500
k (W/m K)	0.252	400	429
$\beta \times 10^{-5}\left(\frac{1}{K}\right)$	65	1.67	1.89

Hybrid nanofluids are a very new concept. The composition of multi-variant dispersed nano-level particles in the base fluids. The nanoparticles used in this investigation are Cu and Ag. Each nanoparticle has a thermal capacity value (C_p), weight density (ρ), thermal conductivity (k), and thermal expansion coefficient (β) as shown in Table 1.

3 Keller-box second-order convergent scheme

Available numerical strategies for obtaining non-similar solutions to the presented issue include the characteristics method, firing technique, explicit and implicit finite differences method, finite element and volume methodologies, and implicit box structures. The box approach provided by Keller [40] is used in this work and is implemented in the MATLAB program. The Keller-box approach is unconditional, stabilized, and accurate to the second order. The work of Vajravelu and Prasad [41] contains information on how to implement the Keller-box technique. The author believes that explaining the conventional numerical scheme is beyond the scope of the current research and that the intricacies are not of interest to the readers. Figure 2 provides a schematic representation.

Table 2: Comparison concerning the evaluates of $-\theta'(0)$ with Pr, with established $Q = 0$ and $\phi/\phi_h = 0$

Pr	Ref. [42]	Ref. [43]	Present
72×10^{-2}	0.80876122	0.80876181	0.80876181
1×10^{0}	1.00000000	1.00000000	1.00000000
3×10^{0}	1.92357431	1.92357420	1.92357420
7×10^{0}	3.07314679	3.07314651	3.07314651
10×10^{0}	3.72055436	3.72055429	3.72055429

The reliability of the current scheme's outcomes is evaluated by comparing them to the existing literature [42,43]. The friction factors are calculated with variations in the Prandtl number in Table 2.

Das *et al.* [42] used the RK Fehlberg approach to solve the unsteadiness of dominant formulas. Jamshed *et al.* [43] used the Keller-box approach to solve the present system. When compared to other approaches, Keller-box methodology gives a more precise and reliable answer.

4 Results and discussion

Figure 3 demonstrates the estimation of fluid velocity increments from $f' = 0$ to $(f \approx 1)$. The measurement of the mixed convection constraint is unlikely to be extended, the velocity will rise at that point. This is because when there is noticeable buoyancy on free convection, mixed convection happens. Subsequently, on the off chance that the estimation of the mixed convection constraints is amplified, at that point, the buoyancy force will increase. As buoyancy develops, at that point, the flow velocity increases.

Figure 4 demonstrates that the thermal effects of the fluid flow diminish from $\theta = 1$ to $\theta \approx 0$ as the estimation of η increments. On the off chance that the estimation of the mixed convection constraint is elevated, at that

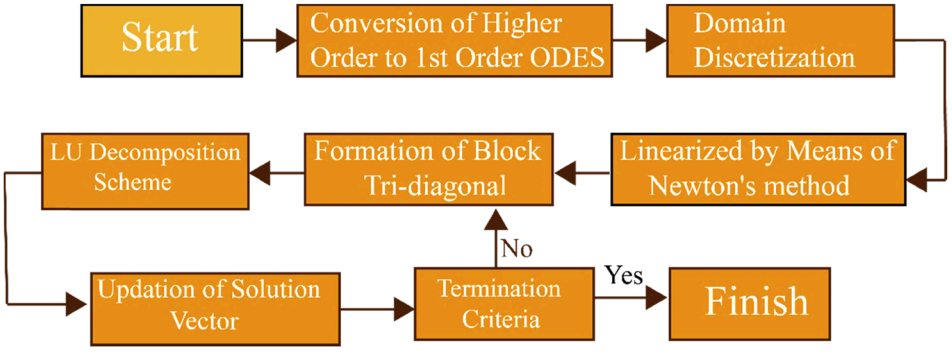

Figure 2: Diagram of clarifying Keller-box scheme.

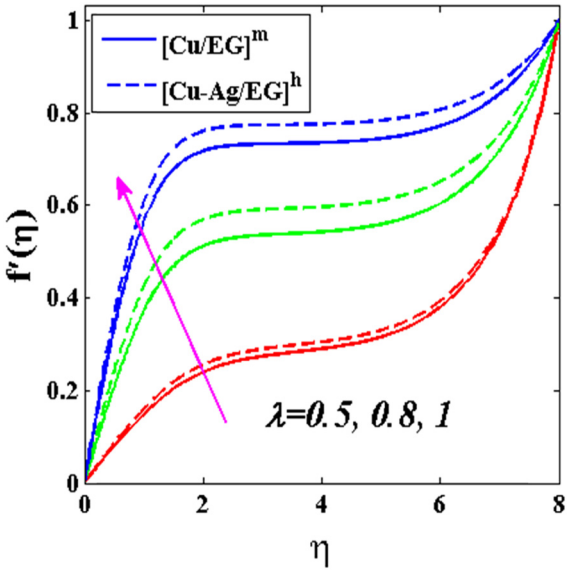

Figure 3: Flow behaviors (f') for the mixed convection constraint variation (λ).

point, the heat will diminish. In this investigation, the mixed convection constraint (λ) is inversely proportional to the heat source constraint (Q), which is numerically defined by $Q = \frac{aQ_0}{U_\infty(\rho C_p)_{hnf}\sqrt{\lambda}}$. The higher the mixed convection value (λ), there is a deceleration in the thermal source (Q). This favors the thermal transferring process of hybrid nanofluids, and it reflects in the reduction of the thermal state in the system for a lower heat source.

Figure 5 shows a fluid flow rate decrease as the Prandtl number value increases. Mathematically, the Prandtl number is the proportion of viscosity to the diffusivity of fluid heat

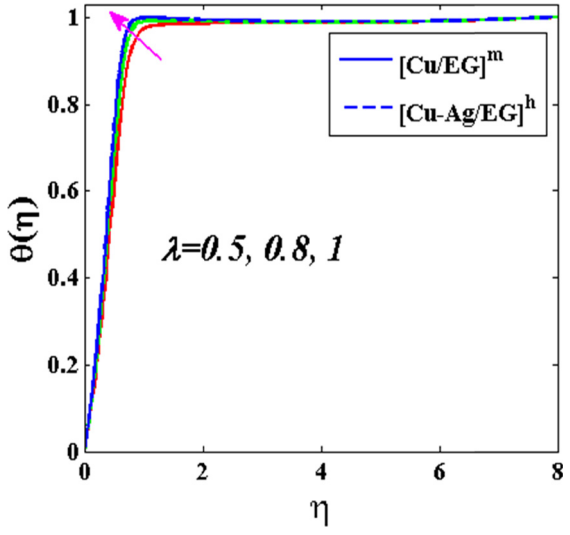

Figure 4: Thermal dispersal (θ) for the mixed convection constraint variation (λ).

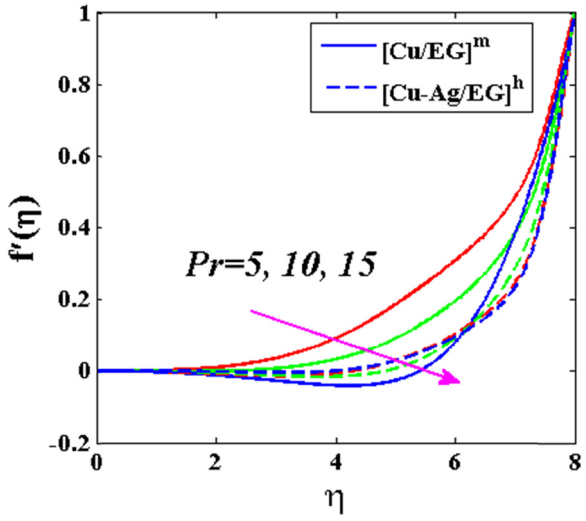

Figure 5: Flow behaviors (f') for the Prandtl number (Pr) variation.

$\left(\mathrm{Pr} = \frac{\nu_f}{\alpha_f}\right)$. As the amount of Prandtl number rises, the kinematic viscosity reduces, and the liquid increases in terms of reducing the fluid flow rate. Figure 6 shows that the higher the amount of the Prandtl, the quicker the temperature falls. This is due to the growing Prandtl number; the thermal conductivity then decreases so that the surface of the sheet develops temperature quicker than the fluid.

Figure 7 establishes that the velocity distribution of the fractional size of nanomolecules rises for the varying ϕ_h as it increases. The values of ϕ_h ($0.01 \le \phi_h \le 0.05$) are going down if the value of ϕ_2 is reduced which is decreased the velocity profile variation due to the hybrid-nanofluids viscosity impact. The higher the χ value, the higher the fluid's viscosity. The larger the fluid's viscosity, the higher the friction between the fluid particles, which

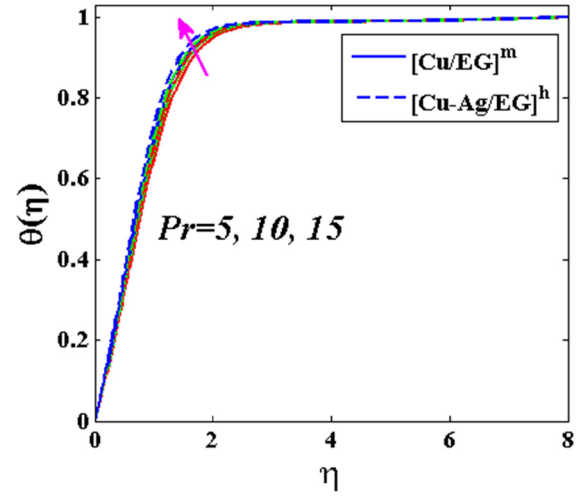

Figure 6: Thermal dispersal (θ) for the Prandtl number (Pr) variation.

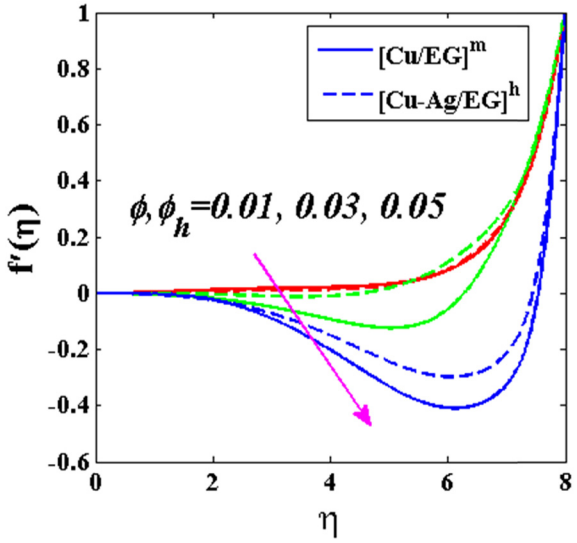

Figure 7: Flow behaviors (f') for the fractional volume variation (ϕ) for normal fluid and (ϕ_h) for the hybrid version of fluid.

triggers the stream velocity to increase while the varying ϕ_1 is increased by $0.1 \le \phi_1 \le 0.15$ and the velocity declines if the ϕ_h value is set to $0.01 \le \phi_h \le 0.05$.

Figure 8 illustrates that the thermal state drops from $\theta = 1$ to $\theta \approx 0$ as the significance of η rises. If the value of the volume of the portion is greater, then the temperature will automatically rise. This phenomenon is because of an increment in the concentration of hybrid nanofluids with a higher value of ϕ. So, if there is friction amid the nanoparticles inside, then the fluid tends to heat which sets the perfect platform for the thermal state of the flowing fluid to rise.

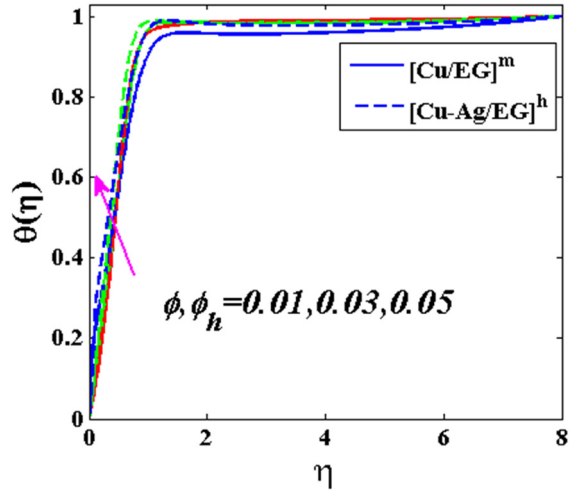

Figure 8: Thermal dispersal (θ) for the fractional volume variation (ϕ) for normal fluid and (ϕ_h) for the hybrid version of fluid.

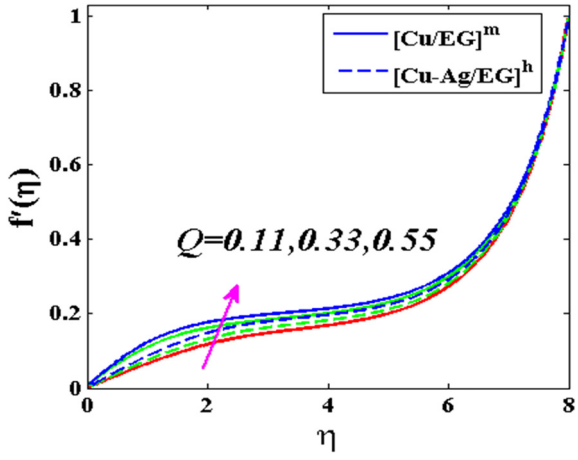

Figure 9: Flow behaviors (f') for the thermal source constraint variation (Q).

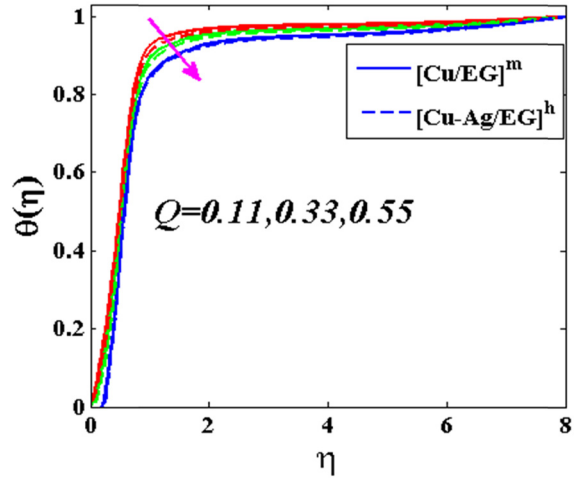

Figure 10: Thermal dispersal (θ) for the thermal source constraint variation (Q).

As the nanoparticles' friction is getting quicker for the raising Q variant values, the fluidity of flowing hybrid nanofluids gets boosted *via* the surface which can be evident in Figure 9. Figure 10 confirms that the temperature improves as the Q value rises. This is because the original heat source Q_0 is increased. For the growing value of Q_0, the heat produced by the hybrid nanofluids is also higher, thus the fluid temperature rises.

5 Conclusion

The outcomes from the investigation are that the fluidity gets enhanced and the thermal dispersal gets reduced as the mixed convection constraint rises. Both the flow

behavior and thermal dispersal decline for higher variation of Prandtl numbers. The hybrid nanofluid flowing gets improved with the volume variation of nanoparticles when $0.01 \le \phi \le 0.05$ and while the flow speed profile with $0.01 \le \phi_{\mathrm{h}} \le 0.05$ is decreased. The dispersal of temperature enhances when the nanoparticles volume constraint in nanofluid are improved. The improving of the heat source boosts the flow velocity and thus raises the heat transport efficiency of the hybrid nanofluid flow in the system. The future scope of this work could be the analysis of various hybrid combinations of fluids that pass over numerous shapes under different circumstances. Further, the present methodology might be utilized in several real and mechanical difficulties [44–49].

Funding information: This work was funded by the Deputyship of Research & Innovation, Ministry of Education in Saudi Arabia, through project number 804/Research Group Program-1. In addition, the authors would like to express their appreciation for the support provided by the Islamic University of Madinah.

Author contributions: All authors have accepted responsibility for the entire content of this manuscript and approved its submission.

Conflict of interest: The authors state no conflict of interest.

Data availability statement: All data generated or analyzed during this study are included in this published article.

References

[1] Crane LJ. Flow past a stretching plate. J Appl Math Phys. 1970;21:645–7.
[2] Ur Rasheed H, AL-Zubaidi A, Islam S, Saleem S, Khan Z, Khan W. Effects of Joule heating and viscous dissipation on magnetohydrodynamic boundary layer flow of Jeffrey nanofluid over a vertically stretching cylinder. Coatings. 2021;11(3):353.
[3] Ahammad NA, Ur Rasheed H, El-Deeb AA, Almarri B, Shah NA. A numerical intuition of activation energy in transient micropolar nanofluid flow configured by an exponentially extended plat surface with thermal radiation effects. Mathematics. 2022;10(21):4046.
[4] Hamilton RL, Crosser OK. Thermal conductivity of heterogeneous two component systems. EC Fundam. 1962;1:187–91.
[5] Maxwell JC. A treatise on electricity and magnetism. 2nd edn. Cambridge: Oxford University Press; 1904. p. 435–41.
[6] Choi SUS. Enhancing thermal conductivity of fluids with nanoparticles. ASME Fluids Eng Div. 1995;231:99–105.
[7] Khan W, Pop I. Boundary-layer flow of a nanofluid past a stretching sheet. Int J Heat Mass Transf. 2010;53:2477–83.
[8] Mabood F, Shateye S, Rashidi MM, Momoniat E, Freidoonimehr N. MHD stagnation point flow heat and mass transfer of nanofluids in porous medium with radiation, viscous dissipation and chemical reaction. Adv Powder Technol. 2016;27:742–9.
[9] Hayat T, Qayyum S, Imtiaz M, Alsaedi A. Comparative study of silver and copper water nanofluids with mixed convection and non-linear thermal radiation. Int J Heat Mass Transf. 2016;102:723–32.
[10] Hayat T, Imtiaz M, Alsaedi A, Kutbi MA. MHD three dimensional flow of nanofluid with velocity slip and non-linear thermal radiation. J Magn Magn Mater. 2015;396:31–7.
[11] Du M, Tang GH. Plasmonic nanofluids based on gold nanorods/nanoellipsoids/nanosheets for solar energy harvesting. Sol Energy. 2016;137:393–400.
[12] Du M, Tang GH. Optical property of nanofluids with particle agglomeration. Sol Energy. 2015;122:864–72.
[13] Rasheed HU, Islam S, Abbas T, Yassen MF. Analytical evaluation of magnetized nanofluid flow in a stagnation point with chemical reaction and nonlinear radiation effect configured by an extended surface. J Appl Math Mech. 2022;103(2):e202200234.
[14] Uddin MJ, Bég OA, Ismail AI. Multiple slip effects on nanofluid dissipative flow in a converging/diverging channel: A numerical study. Heat Transf. 2021;51:1040–61.
[15] Uddin MJ, Bég OA, Ismail AI. Radiative convective nanofluid flow past a stretching/shrinking sheet with slip effects. J Thermo Phy Heat Trans. 2015;29(3):4372.
[16] Anjali Devi SP, Devi SUS. Numerical investigation of hydromagnetic hybrid Cu– Al_2O_3/water nanofluid flow over a permeable stretching sheet with suction. Int J Nonlinear Sci Numer Simul. 2016;17(5):249–57.
[17] Devi SUS, Anjali Devi SP. Numerical investigation of three-dimensional hybrid Cu–Al_2O_3/ water nanofluid flow over a stretching sheet with effecting Lorentz force subject to Newtonian heating. Can J Phys. 2016;94(5):490–6.
[18] Eid MR, Nafe MA. Thermal conductivity variation and heat generation effects on magneto-hybrid nanofluid flow in a porous medium with slip condition. Waves Random Complex Media. 2022;32(3):1103–27. doi: 10.1080/17455030.2020.1810365.
[19] Takabi B, Salehi S. Augmentation of the heat transfer performance of a sinusoidal corrugated enclosure by employing hybrid nanofluid. Adv Mech Eng. 2014;6:147059.
[20] Jamshed W, Prakash M, Devi SS, Ibrahim RW, Shahzad F, Nisar KS, et al. A brief comparative examination of tangent hyperbolic hybrid nanofluid through a extending surface: numerical Keller–Box scheme. Sci Rep. 2021;11:24032.
[21] Redouane F, Jamshed W, Suriya Uma Devi S, Prakash M, Nisar KS, Nasir NA, et al. Galerkin finite element study for mixed convection (TiO_2–SiO_2/water) hybrid-nanofluidic flow in a triangular aperture heated beneath. Sci Rep. 2021;11:22905.
[22] Eastman JA, Choi SUS, Li S, Yu W, Thompson LJ. Anomalously increased effective thermal conductivities of ethylene glycol-based nanofluids containing copper nanoparticles. Appl Phys Lett. 2001;78(6):718–20.

[23] Suresh S, Venkitaraj KP, Selvakumar P, Chandrasekar M. Synthesis of Al2O3–Cu/water hybrid nanofluid using two step method and its thermo physical properties. Colloids Surf A Physicochem Eng Asp. 2011;388(1–3):41–8.
[24] Suresh S, Venkitaraj KP, Hameed MS, Sarangan J. Turbulent heat transfer and pressure drop characteristics of dilute water based Al2O3–Cu hybrid nanofluids. J Nanosci Nanotechnol. 2014;14(3):2563–72.
[25] Sarkar J, Ghosh P, Adil A. A review on hybrid nanofluids: recent research, development and applications. Renew Sust Energy Rev. 2015;43:164–77.
[26] Hassan M, Marin M, Ellahi R, Alamri SZ. Exploration of convective heat transfer and fow characteristics synthesis by Cu–Ag/water hybrid-nanofluids. Heat Transf Res. 2018;49(18):1837–48.
[27] Dinarvand S, Pop I. Free-convective flow of copper/water nanofluid about a rotating down-pointing cone using Tiwari-Das nanofluid scheme. Adv Powder Technol. 2017;28(3):900–9.
[28] Acharya N. On the flow patterns and thermal control of radiative natural convective hybrid nanofluid flow inside a square enclosure having various shaped multiple heated obstacles. Eur Phys J Plus. 2021;136(8):889.
[29] Acharya N. On the hydrothermal behavior and entropy analysis of buoyancy driven magneto-hydrodynamic hybrid nanofluid flow within an octagonal enclosure fitted with fins: Application to thermal energy storage. J Energy Storage. 2022;53:105198.
[30] Acharya N, Chamkha AJ. On the magneto-hydrodynamic Al_2O_3-water nanofluid flow through parallel fins enclosed inside a partially heated hexagonal cavity. Int Commun Heat Mass Transf. 2022;132:105885.
[31] Khan U, Ahmad S, Hayyat A, Khan I, Nisar KS, Baleanu D. On the Cattaneo-Christov heat flux model and OHAM analysis for three different types of nanofluids. Appl Sci. 2020;10(3):886.
[32] Waini I, Ishak A, Pop I. Transpiration effects on hybrid nanofluid flow and heat transfer over a stretching/shrinking sheet with uniform shear flow. Alex Eng J. 2020;59(1):91–9.
[33] Ahmad S, Nadeem S. Application of CNT-based micropolar hybrid nanofluid flow in the presence of Newtonian heating. Appl Nanosci. 2020;10:1–13.
[34] Lund LA, Omar Z, Khan I, Seikh AH, Sherif EM, Nisar KS. Stability analysis and multiple solution of Cu–Al_2O_3/H_2O nanofluid contains hybrid nanomaterials over a shrinking surface in the presence of viscous dissipation. J Mater Res Technol. 2020;9(1):421–32.
[35] Waini I, Ishak A, Pop I. Hybrid nanofluid flow past a permeable moving thin needle. Mathematics. 2020;8(4):612.
[36] Mozafari S, Li W, Dixit M, Seifert S, Lee B, Kovarik L, et al. The role of nanoparticle size and ligand coverage in size focusing of colloidal metal nanoparticles. Nanoscal Adv. 2019;1(10):4052–66.
[37] Amirsom NA, Uddin M, Basir MFM, Ismail A, Bég OA, Kadir A. Three-dimensional bioconvection nanofluid flow from a bi-axial stretching sheet with anisotropic slip. Sains Malays. 2019;48(5):1137–49.
[38] Ali F, Awais M, Ali A, Vrinceanu N, Shah Z, Tirth V. Intelligent computing with Levenberg–Marquardt artificial neural network for Carbon nanotubes-water between stretchable rotating disks. Sci Rep. 2023;13(1):3901.
[39] Tang T-Q, Rooman M, Shah Z, Jan MA, Vrinceanu N, Racheriu M. Computational study and characteristics of magnetized gold-blood Oldroyd-B nanofluid flow and heat transfer in stenosis narrow arteries. J Magn Magn Mater. 2023;569:170448.
[40] Keller HB. A new difference scheme for parabolic problems. In: Hubbard B, editor. Numerical Solutions of Partial Differential Equations. Vol. 2. New York: Academic Press; 1971. p. 327–50.
[41] Vajravelu K, Prasad K. Keller-box method and its application. Berlin, Germany: De Gruyter; 2014.
[42] Das S, Chakraborty S, Jana RN, Makinde OD. Entropy analysis of unsteady magneto-nanofluid flow past accelerating stretching sheet with convective boundary condition. Appl Math Mech. 2015;36(2):1593–610.
[43] Jamshed W, Uma Devi SS, Safdar R, Redouane F, Nisar KS, Eid MR. Comprehensive analysis on copper-iron (II, III)/oxide-engine oil Casson nanofluid flowing and thermal features in parabolic trough solar collector. J Taibah Univer Sci. 2021;15(1):619–36.
[44] Jamshed W, Nisar KS, Ibrahim RW, Mukhtar T, Vijayakumar V, Ahmad F. Computational frame work of Cattaneo-Christov heat flux effects on Engine Oil based Williamson hybrid nanofluids: A thermal case study. Case Stud Therm Eng. 2021;26:101179.
[45] Jamshed W, Eid MR, Al-Hossainy AF, Raizah Z, Tag El Din ESM, Sajid T. Experimental and TDDFT materials simulation of thermal characteristics and entropy optimized of Williamson Cu-methanol and Al_2O_3-methanol nanofluid flowing through solar collector. Sci Rep. 2022;12:18130.
[46] Tang T-Q, Rooman M, Vrinceanu N, Shah Z, Alshehri A. Blood flow of Au-nanofluid using Sisko model in stenotic artery with porous walls and viscous dissipation effect. Micromachines. 2022;13(8):1303.
[47] Shahzad F, Jamshed W, Eid MR, El Din SM, Banerjee R. Mathematical modelling of graphene-oxide/kerosene oil nanofluid *via* radiative linear extendable surface. Alex Eng J. 2023;70:395–410.
[48] Dawar A, Islam S, Shah Z, Lone SA. A comparative analysis of the magnetized sodium alginate-based hybrid nanofluid flows through cone, wedge, and plate. ZAMM-J Appl Math Mech. 2023;103(1):e202200128.
[49] Ullah I, Ali F, Isa SM, Murtaza S, Jamshed W, Eid MR, et al. Electro-magnetic radiative flowing of Williamson-dusty nanofluid along elongating sheet: Nanotechnology application. Arab J Chem. 2023;16(5):104698.